

# Effect of Ni Concentration in Cu-Fe-Ni Alloys Coating on Mild Steel Substrate Prepared by Electrochemical Deposition

Abbas Ayoub, Naseeb Ahmad\*, Muhammad Haseeb-U-Rehman, Muhammad Abbas

Department of Physics, Khwaja Fareed University of Engineering and Information Technology, Rahim Yar Khan, Pakistan

## Email address:

abbasayoub2365@gmail.com (Abbas Ayoub), naseeb.ahmad@kfueit.edu.pk (Naseeb Ahmad),

haseeb.khanhk1992@gmail.com (Muhammad Haseeb-U-Rehman), aeoabbas@gmail.com (Muhammad Abbas)

\*Corresponding author

## To cite this article:

Abbas Ayoub, Naseeb Ahmad, Muhammad Haseeb-U-Rehman, Muhammad Abbas. Effect of Ni Concentration in Cu-Fe-Ni Alloys Coating on Mild Steel Substrate Prepared by Electrochemical Deposition. *Science Development*. Vol. 4, No. 3, 2023, pp. 42-48.

doi: 10.11648/j.scidev.20230403.12

**Received:** April 14, 2023; **Accepted:** August 28, 2023; **Published:** September 13, 2023

---

**Abstract:** Mild steel has applications in construction, mechanical engineering, general-purpose fabrication, fencing, furniture components for different shapes, and other industries. Cu-Fe-Ni alloy coating with different concentrations of Ni was produced on low carbon steel substrate by electrodeposition in this research. Electrochemical deposition (also known as electrodeposition) is one of the most commonly used techniques for the preparation of adherent metallic coatings used to improve the different properties of the base material. The electrolytic bath contained the  $31.92 \text{ g l}^{-1}$   $\text{CuSO}_4$ ,  $54.2 \text{ g l}^{-1}$   $\text{FeSO}_4$ ,  $\text{NiSO}_4 \cdot 7\text{H}_2\text{O}$  ( $0.00 \text{ g l}^{-1}$ ,  $14.04 \text{ g l}^{-1}$ ,  $28.08 \text{ g l}^{-1}$ ,  $42.12 \text{ g l}^{-1}$ ) and  $15.4 \text{ g l}^{-1}$   $\text{H}_3\text{BO}_3$  as buffer to maintain pH at 3. The electrodeposition is done at suitable deposition parameters. The effect of Ni concentration on the surface morphology, structure, and mechanical properties of the coating was revealed by scanning electron microscope (SEM), X-ray diffraction (XRD) analysis with a 45 kV accelerating voltage and a 40 mA current, and Vicker hardness tester respectively. Obtained results showed that with the increase in Ni content, grain size increases from 65.898 nm to 94.770 nm and elongation decreases from 39.780% to 37.033% while the mechanical properties increase. The thickness of deposited Cu-Fe-Ni alloys has a decreasing trend of thickness with increasing Ni contents. The coating thickness decreased from 82.73  $\mu\text{m}$  to 34.98  $\mu\text{m}$ .

**Keywords:** Electrodeposition, Nickel, X-Ray Diffraction, Cu-Ni Alloys, Mild Steel Substrate

---

## 1. Introduction

Nickel-copper alloys are extremely popular due to their excellent corrosion resistance in both acidic and alkaline environments [1–5]. The conventional Monel (70Ni-30Cu) is reported to have remarkable resistance to corrosion in flowing seawater, which makes it a highly suitable material for marine applications [1, 6–7]. However, due to its higher cost, conventional cast Monel is not always feasible to use as a bulk material. Ni-Cu alloy coatings on steel are known to have a lot of potential for replacing Monel as a bulk material. These coatings have several applications in marine structures [8].

Electrochemical deposition (also known as electrodeposition) is one of the most commonly used techniques for the preparation of adherent metallic coatings used to improve the different properties of the base material

[1]. Electrodeposited coatings are not only applied in order to protect the metal substrate from corrosion but also to impart a decorative appearance, enhance wear resistance, improve electrical properties and solder ability, etc. [2]. Nickel is one of the most widely used coatings in automotive, aerospace, and surface engineering for both decorative and functional purposes. Electrodeposition technology offers new prospects in the microelectronic fabrication businesses these days. The characteristics and morphology of deposits are significantly influenced by the electrodeposition conditions.

The electrodeposition of Fe-Co alloys in different solutions has been discovered for nearly two decades [3–5]. Several additives get considerable attention due to their positive influence on electrolytic bath stability and the quality of the deposition which forms during the process. The most frequently used additive to improve the features of the

Fe group alloys is saccharin [6-8]. As it tends to reduce the tensile strength and improve grain size and roughness [9]. The experiments show that during the process of electroplating, the Sulphur atom present in the sulphone group of sodium saccharin reduces sulfide ions during the electrochemical process which incorporates itself into the deposits [10]. Sodium propargyl sulfonate has been proven to be a good addition for the reduction of internal stresses and the refinement of grains in the Fe-Co deposits. Internal forces appear to be an important source of coercion. Lower coercivity is usually equated to reduced stress [11]. On the contrary, no electrodeposition of Fe-Co alloy in Sodium propargyl sulfonate solution has been formed yet.

Fe-Ni alloys have the lowest thermal expansion coefficient and strong magnetic performance [12]. Hence, Fe-Ni alloys have wider common usage in today's evolving and expanding heavy industries of aerospace, electronics, and machine building (mechanics). Because of their better deposition quality, fast productivity, and low cost, the technology of electrodeposition offers new scenarios in electronic fabrication businesses. e.g. it has been widely used in recording heads to deposit magnetic alloy on them [13]. Different types of alloys are formed to have greater tensile strength than their metals themselves. Hence, there is always a greater and ever-increasing use of various kinds of alloys in the modern-day's metal industry. The common use of stainless steel is in household products and construction machinery [14].

It was found that adjusting parameters highly impact mechanical properties. Previous literature reported that the amount of materials that have been used to manufacture industrial parts is mild steel. However, few researchers [21, 22] have investigated the effect of alloying elements on the microstructure and mechanical properties of as-deposited components fabricated by additive manufacturing. The nickel element is an austenite-forming element, which leads to the formation of the face-centered cubic phase. Mild steel has applications in construction, automobiles, mechanical engineering, general purpose fabrication, fencing, cages, frames, furniture components for different shapes, pipelines, fences for businesses and homes, and other industries, but it has weak mechanical properties, degrades and corrodes easily. To cover these problems, we use Ni in Cu-Fe alloy because Ni has all the properties related to that problem. Nickel is very important and widely used in alloy steels. It is ideal for a solid solution to make strengthened, a

hardenability agent, and very important to promote high toughness at low temperatures. Ni helps to cover corrosion, heat resistance, and scratches. Ni also increases the elastic limit of mild steel. When Ni alloy is coated on steel, its hardness, and density increase. It also improves resistance to corrosion and oxidation. Hence, if we coat Cu-Fe alloy with different concentrations of Ni it covers most of the problems that we face in mild steel.

## 2. Materials and Methodology

Electro deposition is the method used to deposit film in our study, preferred due to its various advantages over the other commonly used methods. It works on the principle of electrolysis, which uses an electric current to remove cations of a probable substance from a solution and coat the substrate in a film. Because of its reliability and low cost, electro-deposition is favored over competing methods. It's a good approach because it doesn't need any temperature or pressure changes. Furthermore, this technique maintains the ability to coat irregular geometrical surfaces and has strong control over its parameters. It's one of the surface plating techniques that can be used for both decorative and practical purposes. It also maintains appearance, extends life, and improves material properties.

Sheets of mild steel having an area of 1 cm<sup>2</sup> were taken for sample preparation. The substrate of 1 cm width has been cut from a mild steel sheet with the help of a die machine. The mild steel substrate was materially polished with increasing first-rate grades of emery paper before electro-deposition. The substrate was then washed with distilled water, then washed with ethanol, dried, and then its weight was measured by digital electronic weight balance.

Four different plating baths were prepared to contain NiSO<sub>4</sub>, FeSO<sub>4</sub>, and CuSO<sub>4</sub>. All baths were prepared at 40°C. FeSO<sub>4</sub> and CuSO<sub>4</sub> concentrations were kept constant at 31.92 g l<sup>-1</sup> in all four baths, while NiSO<sub>4</sub> concentration varied as 0 g l<sup>-1</sup>, 14.04 g l<sup>-1</sup>, 28.08 g l<sup>-1</sup>, and 42.12 g l<sup>-1</sup>. The salts were dissolved in distilled water by magnetically stirring at various r. p. m. on a hot plate. The low nickel content in the baths was taken to ensure diffusion-controlled deposition of nickel. 15.4 g l<sup>-1</sup> boric acid was added to the solution as a buffer. 2.5 g l<sup>-1</sup> saccharin was used to maintain the pH of the solution. The pH of the baths was adjusted to 3. All chemicals used were of laboratory grade.

*Table 1. Bath compositions for electrodeposition of all samples.*

Bath Composition	Concentration (g l <sup>-1</sup> )				Operating Parameters
	Bath A	Bath B	Bath C	Bath D	
CuSO <sub>4</sub>	31.92	31.92	31.92	31.92	pH = 3
FeSO <sub>4</sub>	54.2	54.2	54.2	54.2	Temperature 40°C
NiSO <sub>4</sub>	0	14.04	28.08	42.12	Current density = 80 mA cm <sup>-2</sup>
H <sub>3</sub> BO <sub>3</sub>	15.4	15.4	15.4	15.4	Saccharin = 2.5 g l <sup>-1</sup>

Electrodeposition experiments were carried out for all four baths in galvanostatic mode. The bath composition and operating parameters for electrodeposition are given in Table 1. The anode was placed on the front side of the cathode to

maintain uniformity of coating on one side of the steel substrate. Magnetic stirring was also employed for good mixing before each experiment, samples were rinsed with distilled water, and electrodeposition was carried out

immediately to ensure no oxide film formed on the surface before deposition.

Masses of the dried substrates were measured by a weight balance (Sartorius BSA 224S-CW) before and after the deposition. The initial mass was subtracted from the final mass to get the current mass of the coating. This mass was used in the calculation of the thickness of the coating. Scanning electron microscopy was performed using a FESEM (Carl Zeiss AG - Supra 25) to understand the coating surface morphology and microstructure. The XRD patterns were obtained using an X-ray source with a 45 kV accelerating voltage and a 40 mA emission present.

### 3. Results and Discussion

#### 3.1. Thickness of Coating

The thickness of the deposited alloy was calculated by using the following “(1)”.

$$t = m / (A \rho_{av}) \quad (1)$$

Where ‘t’ is the thickness of the deposited material and ‘m’ is the mass that is deposited on the substrate and ‘A’ is the area of deposited material and ‘ $\rho$ ’ is the average density of the deposited alloy. The data obtained from “(1)” is given in Table 2.

**Table 2.** Deposited mass and thickness of Cu-Fe-Ni coating.

Sample No.	Concentration of Ni (g)	Mass difference (g)	Thickness ( $\mu\text{m}$ )
1	0.00	0.07	82.73
2	2.93	0.06	70.51
3	5.86	0.03	35.10
4	8.79	0.03	34.98

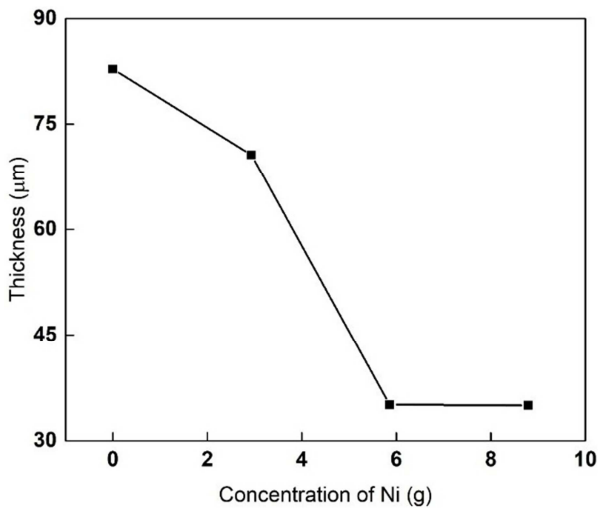


**Figure 1.** Concentration of Ni versus the thickness of the coating Cu-Fe-Ni alloy.

A graph is drawn between the thickness of an investigated alloy and different Ni concentrations as shown in Figure 1.

The calculated thickness for samples shows a continuous decrease from 82.73  $\mu\text{m}$  to 34.98  $\mu\text{m}$  for samples 1-4. The initial thickness is limited to 82.73  $\mu\text{m}$  in sample 1. An increase in Ni content in the electrolyte decreases the average thickness in sample 4 which is 34.98  $\mu\text{m}$ . In the same electrodeposition conditions, a sudden decline was observed between samples 2 and 3 wherein coating thickness decreased almost 2 times. It is because less mass is deposited on the surface. The decrease in thickness could be related to a decrease in deposition mass [16].

#### 3.2. Structure Determination and Phase Analysis of Coated Alloys

An X-ray diffractometer is used to determine the lattice parameters, phase structure, and grain size of binary Cu-Fe as well as ternary Cu-Fe-Ni alloys. Results obtained from X-ray diffraction analysis are given in Table 3.

**Table 3.** Structure parameters obtained from XRD data for Cu-Fe-Ni alloys.

Sample No	2 $\theta$ (degrees)	Lattice Constant ( $\text{\AA}$ )	Miller indices (hkl)	Crystallite size (nm)	Crystal structure
1	43.408	3.607507	(111)	30.503	FCC
	50.445		(200)		
	73.799		(220)		
2	43.242	3.609442	(111)	65.898	FCC
	50.529		(200)		
	74.024		(220)		
3	43.488	3.610944	(111)	81.704	FCC
	50.506		(200)		
	73.714		(220)		
4	43.601	3.611893	(111)	94.770	FCC
	50.737		(200)		
	74.195		(220)		

The effect of Ni concentration on the structure of a ternary alloy Cu-Fe-Ni coating is shown with the XRD patterns in Figure 2. The reflection has a face-centered cubic [17] structure and the crystal planes in all coatings are and (220) at

different  $2\theta$  angles 43.408°, 50.445°, and 73.799° are detected [10, 15, 18-19]. It could be stated that with the addition of Ni, the Ni contents are more deposited in the plane [10]. The specimen might be textured [20, 21].

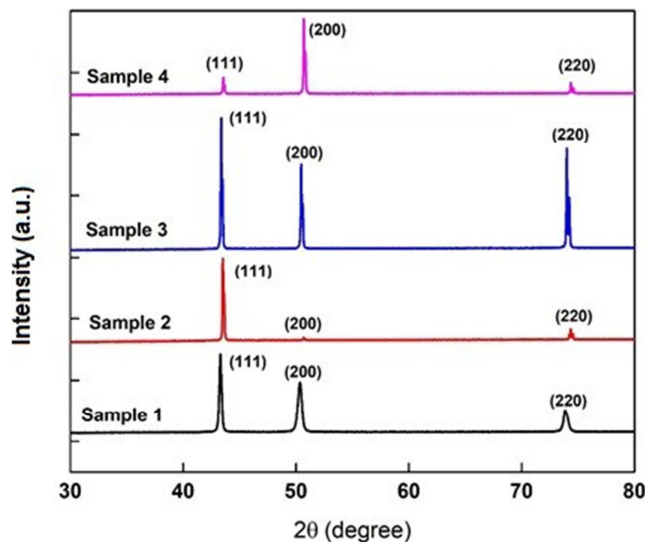


Figure 2. XRD structure for Cu-Fe-Ni coating alloy.

A graph is drawn for crystallite size and the Lattice constant against Ni concentration is shown in Figure 3. From the graph, it is clear that with the increase in Ni concentration, the crystallite size as well as the lattice constant also increases. It is exhibited from the graph that the crystallite size and lattice constant of the first sample are 30.503 nm and 3.6075 respectively when no Ni is added.

Table 4. Crystallite size and lattice constant with different Ni concentrations.

Sample No.	Concentration of Ni (g)	Crystallite size (nm)	Lattice Constant (Å)
1	0.00	30.503	3.6075077
2	2.93	65.898	3.6094425
3	5.86	81.704	3.6109442
4	8.79	94.770	3.6118935

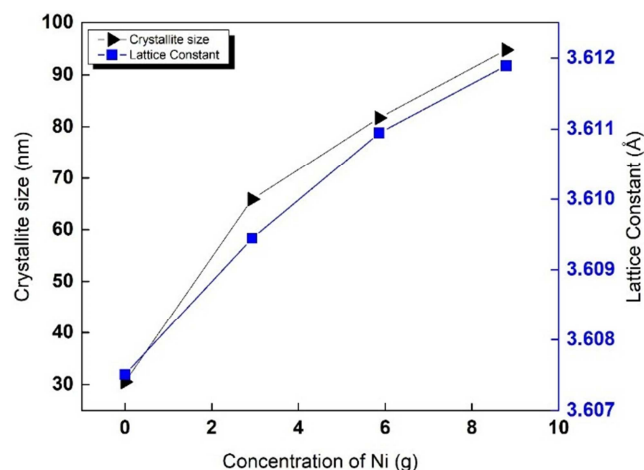


Figure 3. Concentration of Ni versus Lattice Constant.

The crystallite size is increased to greater than 2 times while the lattice constant increases to almost 0.05% when Ni is included for sample 2 and it continuously increases. While for sample 4, the maximum Ni content crystallite size increases by approximately 3 times, while the lattice constant increases approximately 0.12% to sample 1. The increase in lattice

constant can be attributed to the lattice constant of Ni as the lattice constant of Ni is greater than the average lattice parameter of Cu and Fe [22]. While the increase in crystallite size can be attributed to an increase in lattice constant [23].

### 3.3. Morphologies of Cu-Fe-Ni Alloys Coating

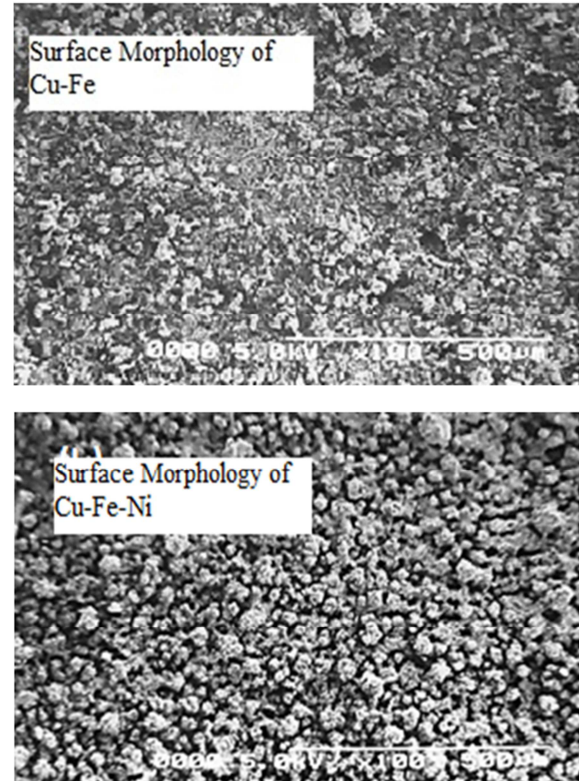


Figure 4. Surface morphology of Cu-Fe-Ni alloys without and with Ni contents.

The influence of electrolyte composition on the surface morphology of coatings is shown in Figure 4 and represents the surface morphology of un-doped  $\text{NiSO}_4$ . The surface of the Cu-Fe coating has a smaller grain size of  $5.66 \mu\text{m}$  with a relatively partial nodule structure. Increasing the Ni concentration significantly affects the surface morphology.

As the Ni content of the alloy increased, the grain size is observed to increase up to  $16.25 \mu\text{m}$  in the Cu-Fe-Ni alloy coatings element and this effect may be caused by the formation of Cu-rich intermetallic before the nucleation of  $\alpha\text{-Fe}$  dendrites [24]. By increasing the Ni content, this small nodule structure also changes to a globular structure [25].

### 3.4. Mechanical Properties

Results of micro-hardness thin films before and after doping of nickel with different concentrations are shown in Table 5.

Ultimate Tensile Stress (UTS) and Micro-hardness data are shown in Table 5. From the graph, it is clear that with the increase in the concentration of nickel, the ultimate tensile stress, as well as the hardness of the material, also increases. It is exhibited from Table 5 that the UTS and hardness of the first sample are 308.499 and 402.835 respectively when no nickel is

added to the solution. Then UTS and hardness increase to almost 3% and 13% when nickel is added to the solution and it continuously increases. While for the last sample of maximum nickel content, UTS, and micro-hardness increase approximately 5% and 24% greater than when nickel is absent

in the deposition. The increase in hardness and UTS must be related to the formation of Cu- and Ni-rich intermetallic. An increase in contiguity in the 3D network may be responsible for the increase in hardness and UTS [26]. These results are following the results reported by Kaya et al [27, 28].

**Table 5.** Ultimate tensile stress and micro-hardness of Cu-Fe-Ni alloy coatings with different concentrations of Ni.

Sample	Concentration of Ni (g)	Mass difference (g)	Thickness ( $\mu\text{m}$ )
Substrate	----	336.022	
Cu-Fe Alloy	0.00	308.499	402.835
	2.93	311.387	454.2465
Cu-Fe-Ni Alloy	5.86	319.433	473.8315
	8.79	325.399	498.9985

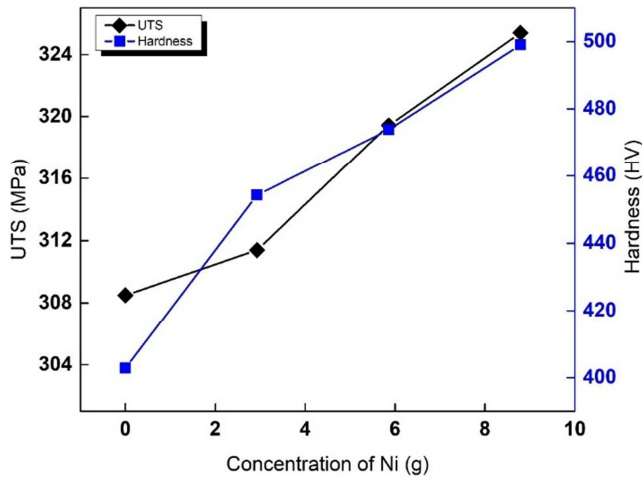


**Figure 5.** Concentration of nickel versus UTS and Micro-hardness of Cu-Fe-Ni alloy coatings.

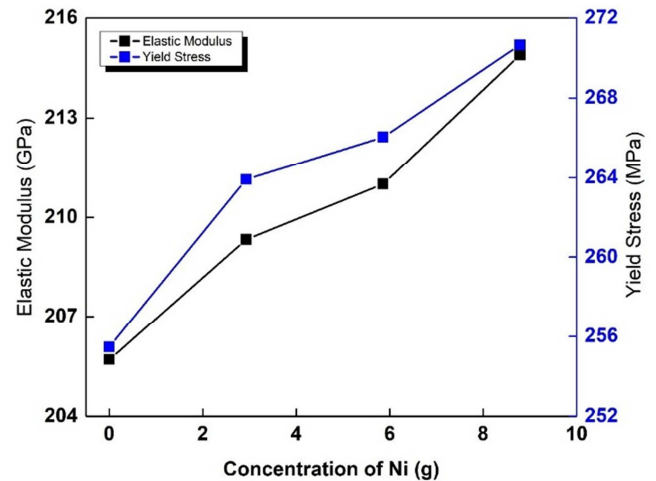


**Figure 6.** Concentration of nickel versus Micro-hardness of Cu-Fe-Ni alloy coatings.

**Table 6.** Elastic modulus and yield stress of Cu-Fe-Ni alloy coatings with different concentrations of Ni.

Sample	Concentration of Ni (g)	Elastic Modulus (GPa)	Yield Stress (MPa)
Substrate	----	200.236	240.922
Cu-Fe Alloy	0.00	205.699	255.470
	2.93	209.330	263.912
Cu-Fe-Ni Alloy	5.86	211.009	266.043
	8.79	214.890	270.656

To clarify the mechanical behavior of the coating, its elastic modulus, and yield stress are taken as a function of nickel content presented in Figure 6. From the graph, it is clear that there is a continuous increment in the elastic modulus and yield stress of the coating. The elastic modulus and yield strength of the substrate are 200.236 GPa and 240.922 MPa respectively, as given in Table 6. But as a Cu-Fe alloy is deposited on the substrate the elastic modulus and yield strength increase to almost 2.7% and 6% respectively. When nickel concentration is added in deposition, this number continuously increases and reaches 7.3% and 12% respectively. It is reflected from the graph that the elastic modulus and yield strength of the sample with the lowest content of nickel are approximately 4.5% and 9% more than the substrate, while the yield strength of the specimen with the highest nickel content reaches 7.3% and 12% respectively, more than the substrate as mentioned earlier. The increase in

coating elastic modulus yield stress can be attributed to the higher elastic modulus and yield stress value of nickel particles with the increase of their contents as compared to other elements, i.e. copper and iron [29, 30].

Results of the Elongation of thin films before and after doping of nickel with different concentrations are shown in Table 7.

**Table 7.** Elongation of Cu-Fe-Ni alloy coatings with different Concentrations of Ni.

Sample	Concentration of Ni (g)	Elongation (%)
Substrate	----	18.987
Cu-Fe Alloy	0.00	39.780
	2.93	38.453
Cu-Fe-Ni Alloy	5.86	37.901
	8.79	37.033



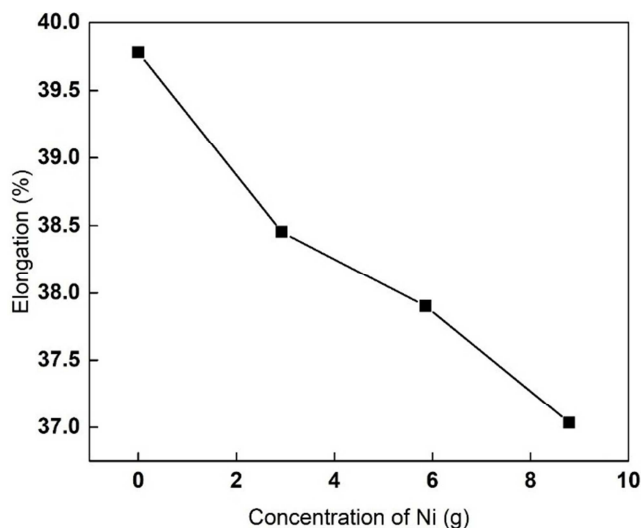


Figure 7. Elongation as a function of Concentration of nickel.

In Figure 7, elongation is taken as a function of nickel content as shown in the graph. From the graph, it is clear that with the increase in the concentration of nickel, the elongation decreases. It is exhibited from the graph that the elongation of the first sample Cu-Fe alloy is 39.780 and decreases continuously. When nickel is added to the deposition, it continuously decreases further. When the first concentration of nickel is  $14.04 \text{ g l}^{-1}$ , as shown in Table 4, is added in the deposition, elongation decreases to 38.453. While as nickel content increases, elongation decreases to 37.033 and these results are under the results reported in the literature [26, 28].

#### 4. Conclusion

In the present study, ternary Cu-Fe-Ni alloys are electrodeposited on a mild steel substrate at suitable operating parameters during electrodeposition. Prepared samples of increasing contents of Ni are studied. In the prepared samples, Crystal structure, surface morphology, and mechanical properties were investigated. The obtained results concluded as the thickness of the coating of the Cu-Fe-Ni alloy on mild steel substrate decreased as Ni concentration increased in solution because the thickness of deposited mass decreased. From the X-ray diffraction results, it is clear that the structure of the crystal is FCC and it is also observed that with the increase in Ni concentration, not only does the lattice constant increase but the crystallite size is also increased because of the lattice constant of Ni as the lattice constant is greater than the average lattice parameter of Cu and Fe. From surface morphology results, it is revealed that with the increase of Ni content in deposition, the grain size of the sample increases. This effect may be caused by the formation of Cu-rich intermetallic before the nucleation of  $\alpha$ -Fe dendrites. It was observed that Ni content in Cu-Fe-Ni alloy on a mild steel substrate increased the mechanical properties of the sample. This improvement could be a result of better properties of Ni.

#### Acknowledgements

It is difficult to overstate my gratitude to my supervisor, Dr. Naseeb Ahmad (Assistant Professor Department of Physics). His sage advice, insightful criticism, sympathetic attitude, enthusiastic supervision especially during experimental work, and patient encouragement aided the writing of this manuscript.

#### References

- [1] Mroz, K., et al., Ni-W electrodeposited coatings on low carbon steel substrate: fatigue observations. *Journal of materials engineering and performance*, 2014. 23 (10): p. 3459-3466.
- [2] Deo, Y., et al., Electrodeposited Ni-Cu alloy coatings on mild steel for enhanced corrosion properties. *Applied Surface Science*, 2020. 515: p. 146078.
- [3] Aguirre, M. d. C., et al., Co100– xFex magnetic thick films prepared by electrodeposition. *Journal of Alloys and Compounds*, 2015. 627: p. 393-401.
- [4] Bento, F. R. and L. H. Mascaro, Analysis of the initial stages of electrocrystallization of Fe, Co and Fe-Co alloys in chloride solutions. *Journal of the Brazilian Chemical Society*, 2002. 13: p. 502-509.
- [5] Yokoshima, T., et al., Preparation of high-B/sub s/Co-Fe soft magnetic thin films by electrodeposition. *IEEE transactions on magnetics*, 2004. 40 (4): p. 2332-2334.
- [6] Brankovic, S. R., Saccharin effect on properties of 2.4 T CoFe films. *Electrochimica acta*, 2012. 84: p. 139-144.
- [7] Brankovic, S. R., R. Haislmaier, and N. Vasiljevic, Physical incorporation of saccharin molecules into electrodeposited soft high magnetic moment CoFe alloys. *Electrochemical and solid-state letters*, 2007. 10 (6): p. D67.
- [8] Lin, Y.-J., et al., Defects, stress and abnormal shift of the (0 0 2) diffraction peak for Li-doped ZnO films. *Applied surface science*, 2010. 256 (24): p. 7623-7627.
- [9] Tabaković, I. and S. Riemer, Roughness development in electrodeposited soft magnetic CoNiFe films in the presence of organic additives. *Journal of the Serbian Chemical Society*, 2003. 68 (4-5): p. 349-361.
- [10] Tabakovic, I., et al., Mechanism of saccharin transformation to metal sulfides and effect of inclusions on corrosion susceptibility of electroplated CoFe magnetic films. *Journal of The Electrochemical Society*, 2006. 153 (8): p. C586.
- [11] Myung, N., et al., Electroformed iron and FeCo alloy. *Electrochimica acta*, 2004. 49 (25): p. 4397-4404.
- [12] Yichun, L., et al., Direct electrodeposition of Fe-Ni alloy films on silicon substrate. *Rare Metal Materials and Engineering*, 2014. 43 (12): p. 2966-2968.
- [13] Czerwinski, F., J. Szpunar, and U. Erb, Structural and magnetic characterization of nanocrystalline Ni-20% Fe permalloy films. *Journal of Materials Science: Materials in Electronics*, 2000. 11 (3): p. 243-251.

- [14] Firouzi-Nerbin, H., F. Nasirpour, and E. Moslehifard, Pulse electrodeposition and corrosion properties of nanocrystalline nickel-chromium alloy coatings on copper substrate. *Journal of Alloys and Compounds*, 2020. 822: p. 153712.
- [15] Abou-Krishna, M., et al., Electrochemical behavior of Zn–Co–Fe alloy electrodeposited from a sulfate bath on various substrate materials. *Arabian Journal of Chemistry*, 2019. 12 (8): p. 3526-3533.
- [16] Taylor, S., *Coatings for corrosion protection: metallic*. 2001.
- [17] Osetsky, Y. N. and D. J. Bacon, Comparison of void strengthening in fcc and bcc metals: large-scale atomic-level modelling. *Materials Science and Engineering: A*, 2005. 400: p. 374-377.
- [18] Abou-Krishna, M., F. Assaf, and S. El-Naby, Electrodeposition and characterization of zinc–nickel–iron alloy from sulfate bath: influence of plating bath temperature. *Journal of Solid State Electrochemistry*, 2009. 13 (6): p. 879-885.
- [19] Schuh, C., T. Nieh, and H. Iwasaki, The effect of solid solution W additions on the mechanical properties of nanocrystalline Ni. *Acta Materialia*, 2003. 51 (2): p. 431-443.
- [20] Wang, L., et al., Microstructure and tribological properties of electrodeposited Ni–Co alloy deposits. *Applied Surface Science*, 2005. 242 (3-4): p. 326-332.
- [21] Chen, L., et al., Influence of pulse frequency on the microstructure and wear resistance of electrodeposited Ni–Al<sub>2</sub>O<sub>3</sub> composite coatings. *Surface and Coatings Technology*, 2006. 201 (3-4): p. 599-605.
- [22] Delhez, R., T. H. De Keijser, and E. Mittemeijer, Determination of crystallite size and lattice distortions through X-ray diffraction line profile analysis. *Fresenius' Zeitschrift für analytische Chemie*, 1982. 312 (1): p. 1-16.
- [23] Kumar, D., M. Singh, and A. K. Singh. Crystallite size effect on lattice strain and crystal structure of Ba<sub>1/4</sub>Sr<sub>3/4</sub>MnO<sub>3</sub> layered perovskite manganite. in *AIP Conference Proceedings*. 2018. AIP Publishing LLC.
- [24] Bogdanoff, T., A. K. Dahle, and S. Seifeddine, Effect of Co and Ni addition on the microstructure and mechanical properties at room and elevated temperature of an Al–7% Si Alloy. *International Journal of metalcasting*, 2018. 12 (3): p. 434-440.
- [25] Sales Amalraj, A., S. Christina Joyce, and A. Joseph Lourdu Rajah, Influence of Ni dopant on surface morphology of nanostructured ZnO thin films grown by SILAR method. *Materials Research Innovations*, 2020. 24 (6): p. 341-348.
- [26] Stadler, F., et al., Effect of main alloying elements on strength of Al–Si foundry alloys at elevated temperatures. *International Journal of Cast Metals Research*, 2012. 25 (4): p. 215-224.
- [27] Kaya, H. and A. Aker, Effect of alloying elements and growth rates on microstructure and mechanical properties in the directionally solidified Al–Si–X alloys. *Journal of Alloys and Compounds*, 2017. 694: p. 145-154.
- [28] Asghar, Z., et al., Three-dimensional study of Ni aluminides in an AlSi12 alloy by means of light optical and synchrotron microtomography. *Acta Materialia*, 2009. 57 (14): p. 4125-4132.
- [29] Vaynman, S., et al., High-strength low-carbon ferritic steel containing Cu–Fe–Ni–Al–Mn precipitates. *Metallurgical and Materials Transactions A*, 2008. 39 (2): p. 363-373.
- [30] Zamani, M., A. Amadeh, and S. L. Baghal, Effect of Co content on electrodeposition mechanism and mechanical properties of electrodeposited Ni–Co alloy. *Transactions of Nonferrous Metals Society of China*, 2016. 26 (2): p. 484-491.